Available online at www.sciencedirect.com
ScienceDirect
Journal of Power Sources 167 (2007) 25–31
JOURNAL OF POWER SOURCES
www.elsevier.com/locate/jpowsour

Hydrogen crossover in high-temperature PEM fuel cells

Xuan Cheng [1], Jianlu Zhang, Yanghua Tang, Chaojie Song, Jun Shen, Datong Song, Jiujun Zhang *

Institute for Fuel Cell Innovation, National Research Council of Canada, Vancouver, BC, Canada V6T 1W5

Received 22 December 2006; received in revised form 5 February 2007; accepted 5 February 2007
Available online 21 February 2007

Abstract

In this paper, hydrogen crossover was measured in an environment of high-temperature proton exchange membrane (PEM) fuel cells using a steady-state electrochemical method at various temperatures (T) (80–120 °C), backpressures (P) (1.0–3.0 atm), and relative humidities (RH) (25–100%). An H_2 crossover model based on an MEA consisting of five layers – anode gas diffusion layer, anode catalyst layer, proton exchange membrane (Nafion 112 or Nafion 117), cathode catalyst layer, and cathode gas diffusion layer – was constructed to obtain an expression for H_2 permeability coefficients as a function of measured H_2 crossover rates and controlled H_2 partial pressures. The model analysis suggests that the dominant factor in the overall H_2 crossover is the step of H_2 diffusing through the PEM. The H_2 permeability coefficients as a function of T, P, and RH obtained in this study show that the increases in both T and P could increase the H_2 permeability coefficient at any given RH. However, the effect of RH on the permeability coefficient seems to be more complicated. The T effect is much larger than that of P and RH. Through experimental data simulation an equation was obtained to describe the T dependencies of the H_2 permeability coefficient, based on which other parameters such as maximum permeability coefficients and activation energies for H_2 crossover through both Nafion 112 and 117 membranes were also evaluated. Both Nafion 112 and Nafion 117 showed similar values of such parameters, suggesting that membrane thickness does not play a significant role in the H_2 crossover mechanism.

Keywords: Proton exchange membrane (PEM) fuel cells; Hydrogen crossover; Permeability coefficient; Temperature; Backpressure; Relative humidity

1. Introduction

Proton exchange membrane (PEM) fuel cells, used as a power source in transportation and stationary applications, have been recognized as the most promising energy converters in terms of high power density, low or zero emissions, and high efficiency [1]. In the last several decades, in order to realize the commercialization of PEM fuel cells, tremendous effort has been put into improving performance and addressing several technology gaps, including high cost and limited reliability and durability. With respect to this effort, property improvements in the membrane electrode assembly (MEA), the heart of a fuel cell in which the converting reactions occur, are the major focus.

An MEA is made up of a cathode, an anode, and a PEM. Their impedances are primarily responsible for the performance loss that occurs during fuel cell operation. For example, fuel cell polarization can be expressed as Eq. (1) [2]

$$V_{\text{cell}} = E^{\text{OCV}} - \eta_{\text{c}} - \eta_{\text{a}} - I_{\text{cell}} R_{\text{m}} \quad (1)$$

where E^{OCV} is the fuel cell open circuit voltage (OCV), I_{cell} the fuel cell current density, R_{m} the MEA resistance dominated by the membrane resistance, and η_{c} and η_{a} are the overpotentials for the cathode and anode, respectively. Among the voltage losses of the cathode (η_{c}), anode (η_{a}), and membrane ($I_{\text{cell}}R_{\text{m}}$), that of the membrane ($I_{\text{cell}}R_{\text{m}}/V_{\text{cell}}$) accounts for about 30% [3]. Reduction in membrane proton resistance is the major approach to reducing membrane voltage loss. One effective and straightforward way to reduce membrane resistance is by using a thinner membrane in the MEA. For example, in early fuel cell development, Nafion 117 with a thickness of 175–183 μm was widely used. Later, Nafion 115 with a thickness of 127 μm was employed, followed by Nafion 112 with a thickness of 51 μm [4], and most recently,

* Corresponding author. Tel.: +1 604 221 3087.
E-mail address: jiujun.zhang@nrc.gc.ca (J. Zhang).
[1] Present address: Department of Materials Science and Engineering, State Key Laboratory for Physical Chemistry of Solid Surfaces, Xiamen University, Xiamen FJ 361005, PR China.

0378-7753/$ – see front matter © 2007 Elsevier B.V. All rights reserved.
doi:10.1016/j.jpowsour.2007.02.027

Nafion 211 or Nafion 111 with a thickness of 25 μm. However, with decreasing the membrane thickness, another problem, fuel (typically, hydrogen) crossover, may become a limited factor, especially when the fuel cell operates at low current densities. Thus, the reduction of H_2 crossover when a thinner membrane is used is a challenge which necessitates the investigation of hydrogen crossover, especially when the fuel cell is operated at higher temperatures at which the H_2 crossover is more severe.

Hydrogen crossover is an undesirable diffusion of hydrogen from the anode to the cathode through the membrane. Hydrogen crossover can have at least three effects, including fuel efficiency reduction, cathode potential depression, and aggressive peroxide radical formation. The hydrogen which crosses over can directly react with oxygen at the cathode surface, resulting in a lower cathode potential than that of a lower fuel cell (OCV), a result confirmed by our recent study of temperature-dependent OCV in PEM fuel cells [5]. More severely, this direct reaction between H_2 and O_2 at the cathode can produce peroxide radicals, which not only attack the catalyst layer but also the membrane, causing significant catalyst-layer and membrane degradation [6]. In addition, it has been confirmed that the formation of hot-points [7] or hydrogen peroxide [8,9] by the highly exothermal chemical reaction between H_2 and O_2 can also lead to pin-holes in membranes, destroying the MEA and causing safety problems. An accelerated sintering of catalysts could be also caused by this hydrogen crossover [6]. Therefore, the measurement of hydrogen crossover, in particular at OCV, at which the most severe crossover occurs, is of importance for the fundamental understanding and practical mitigation of fuel cell degradation and membrane failure.

Since H_2 crossover is a diffusion-controlled process, the PEM structure [10] and fuel cell operating conditions [8,11] can greatly influence the crossover process. For example, it can be expected that the uses of thinner membranes and the operation of fuel cells at high temperature and high pressure will facilitate H_2 crossover. H_2 crossover at temperatures up to 80 °C has been investigated by a method of limiting current, primarily using linear sweep voltammetry (LSV) through various membranes: Nafion [12–15], Nafion-palladium [12], sulfonated poly(ether ether ketone) (SPEEK) [16], and Flemion [17]. It was found that the water content in the membrane [12] and gas pressure [8] had a great effect on the H_2 crossover rate. An in situ method for limiting H_2 crossover current measurements in subscale and full-size single cells has also been developed [18].

High-temperature PEM fuel cells (>80 °C) have several advantages over those operated at lower temperatures [19]. However, the data available for H_2 crossover at temperatures higher than 80 °C are very limited. It can be expected that the problems associated with high-temperature H_2 crossover would be worse than those at lower temperatures. In a recent model study based on previously developed models [20,21], Rama et al. [22] discussed the effects of membrane thickness, operating pressure and temperature, and current density on H_2 crossover using a concentrated solution membrane system containing four species: water, electrolyte membrane, proton and hydrogen. The simulated results indicate that the increase in the H_2 crossover found when temperatures rose from 80 to 100 °C at 3 atm was attributed to the dependence of the H_2 diffusion coefficient on temperature [22]. The use of Nafion-based composite membranes could reduce H_2 crossover with a more crystalline region being provided after heat-treating at 120 °C [23] or with less porosity resulting from well-dispersed small additive particles [24].

The structure and chemistry of PEM are critical in the control of proton and water transport and H_2 crossover. The three-region model [25] and cluster-network model [26] have been widely used to describe the microstructure of perfluorosulfonated membranes such as Nafion-type membranes. However, there is still no agreement as to whether the gas permeates through Nafion in the intermediate region, which consists mainly of the flexible amorphous part of the perfluorocarbon backbone [13,14], or through the hydrated ionic clusters, which contain mainly water and sulfonic acid groups [12]. A compromise solution, that the gas permeates through both regions, has also been suggested [27].

In order to improve our understanding of the H_2 crossover phenomena, it is necessary to obtain more information about H_2 crossover at elevated temperatures and to further clarify the nature of H_2 crossover from the anode to the cathode via the MEA. This investigation was carried out to examine the effects of temperature, pressure, and relative humidity on H_2 crossover. A multilayer diffusion model was proposed to describe H_2 crossover through an MEA. Some H_2 crossover parameters were evaluated with a focus on the high-temperature H_2 crossover behaviour observed in a fuel cell assembling environment.

2. Experimental

The MEA, with an active area of 4.4 cm^2, was prepared by hot pressing the anode, a Nafion 112 (or 117) membrane, and cathode together at 135 °C and 75 kg cm^{-2} for 2 min. The gas diffusion electrode (GDE) was prepared by spraying a homogeneous catalyst ink, consisting of catalyst, Nafion solution, and *iso*-propanol, onto a gas diffusion layer (GDL). This GDL was a PTFE- and carbon-black impregnated carbon paper (Toray, TGP-H-060). E-Tek 20% Pt/Ru/C and 40% Pt/C were used as the anode and cathode catalysts, with a total Pt loading of ~1.0 mg cm^{-2}. The total Nafion loading in the MEA was 1.4 mg cm^{-2}. The Nafion 112 and 117 (DuPont) used for the PEM were treated in 3% H_2O_2 (aq), 1 M H_2SO_4 (aq); rinsed; and then soaked separately in deionized water for 1 h at 60–80 °C, followed by a careful washing with double-distilled water.

An in-house single fuel cell hardware, described in our previous paper [3], was used for measuring fuel cell performance and H_2 crossover. A bladder pressure of 4.4 atm was used to hold the single cell together and provide sufficient electrical contact between the MEA and the graphite bipolar plates. Both graphite plates had the same serpentine flow fields. A 100 W Fideris fuel cell test station controlled by FC Power software and equipped with an in-house modified humidifier which could reach 100% RH at 120 °C was used for fuel cell polarization at different temperatures, pressures, and relative humidities. When the cell was controlled at a certain RH, the H_2 and air (or nitrogen), before they were fed into the anode and cathode, were first

passed through their corresponding humidifiers, in which they were humidified at the same temperature as that of the fuel cell. During all tests, the pressures for both the anode and the cathode sides were kept at the same level.

Before H_2 crossover was measured at various conditions, the fuel cell assembled with an MEA was conditioned at 80 °C, 3 atm, and 100% RH with a load of 1.0 A cm^{-2} for 4 h, followed by a collection of steady-state polarization data in the current density range of 0–2.5 A cm^{-2}. After that, a humidified nitrogen stream was introduced into the cathode to remove the air. After 30 min of N_2 flushing through the cathode, a Solartron 1287 potentiostat was connected to the fuel cell for H_2 crossover measurements, with the working electrode probe connected to the cathode and the counter/reference electrode probes connected together to the anode. A steady-state electrochemical method was used to record the current produced from the oxidation of crossed H_2 from the anode at an applied cathode potential of 0.5 V relative to the potential of the H_2-flushed anode. At this cathode potential, all H_2 that has crossed over from the anode to the cathode should be completely oxidized, giving a current indicative of the amount of hydrogen that has crossed over. The obtained current was defined as $I_{H_2}^{cross}$ (unit: A) for the calculation of H_2 crossover rate ($J_{H_2}^{cross}$, mol cm^{-2} s^{-1}). The following Faraday's equation was used to obtain the H_2 crossover rate:

$$J_{H_2}^{cross} = \frac{I_{H_2}^{cross}}{nFA} \tag{2}$$

where n is the electron number of H_2 oxidation (=2), F the Faraday constant (A s mol^{-1}), and A is the MEA active area (cm^2). It is worthwhile to point out that the H_2 crossover rate measured by this procedure should represent the case at OCV conditions rather than those at load.

In order to obtain the dependencies of the H_2 permeability coefficient ($\psi_{H_2}^{PEM}$) on the temperature (T), fuel cell backpressure (P), and relative humidity (RH), the H_2 partial pressure ($P_{H_2}^a$) as a function of T, P, and RH must be known. The values of the H_2 partial pressure were calculated based on the fuel cell anode inlet total pressure (P_{inlet}^a), the H_2 partial pressure in the inlet stream ($P_{H_2\text{-inlet}}^a$), and the outlet total pressure, which is equal to the backpressure (P). The following Eq. (3) was used to calculate the partial pressure inside the anode chamber by assuming that the pressure drop along the superfine channel is linear:

$$P_{H_2}^a = \left(\frac{P_{H_2\text{-inlet}}^a}{P_{inlet}^a}\right)\left(\frac{P_{inlet}^a + P}{2}\right) \tag{3}$$

where P_{inlet}^a and P can be measured experimentally, and $P_{H_2\text{-inlet}}^a$ can be obtained based on the inlet H_2 stream flow rate, the water vapour partial pressure, and the inlet total pressure (P_{inlet}^a). Note that the amount of H_2 that crosses over from the anode to the cathode during the measurements is expected to be too small to cause a significant drop in the H_2 partial pressure. Therefore, it is not necessary to make a crossover correction to the value of $P_{H_2}^a$. The H_2 partial pressure data obtained according to Eq. (3) at various Ts, Ps, and RHs were used to calculate H_2 permeability coefficients, as discussed in later sections of this paper.

3. Results and discussion

3.1. Theoretical description of the H_2 crossover through the MEA

In a fuel cell, hydrogen crossover usually takes place from the anode side to the cathode side through a MEA, as illustrated in Fig. 1, which schematically represents a typical MEA structure consisting of five layers: anode gas diffusion layer (GDL(a)), anode catalyst layer (CL(a)), proton exchange membrane (PEM), cathode CL (CL(c)), and cathode GDL (GDL(c)). By Fick's first law, the steady-state H_2 crossover rate can be treated as the diffusion through the MEA:

$$J_{H_2}^{cross} = \left(\frac{D_{H_2}}{l}\right)(C_{H_2}^a - C_{H_2}^c) \tag{4}$$

where $C_{H_2}^a$ and $C_{H_2}^c$ are the concentration of H_2 at the interface between the anode H_2 gas phase and the GDL(a) surface, and the concentration at the interface between the cathode air (or nitrogen) gas phase and the GDL(c) surface, respectively. D_H is the overall diffusion coefficient and l is the MEA thickness.

As depicted in Fig. 1, the overall resistance for H_2 diffusion (l/D_{H_2}) through an MEA is the sum of the resistance for H_2 diffusion through each layer. Therefore, D_{H_2} can be expressed as Eq. (5) based on the equivalent resistance of the five layers in series:

$$\frac{l}{D_{H_2}} = \frac{l_{GDL}^a}{D_{GDL}^a} + \frac{l_{CL}^a}{D_{CL}^a} + \frac{l_{PEM}}{D_{PEM}} + \frac{l_{CL}^c}{D_{CL}^c} + \frac{l_{GDL}^c}{D_{GDL}^c} \tag{5}$$

where l_{GDL}^a, l_{CL}^a, l_{PEM}, l_{CL}^c, and l_{GDL}^c are the thicknesses of GDL(a), CL(a), PEM, CL(c), and GDL(c), respectively, and l can be expressed as Eq. (6):

$$l = l_{GDL}^a + l_{CL}^a + l_{PEM} + l_{CL}^c + l_{GDL}^c \tag{6}$$

In (5) D_{GDL}^a, D_{CL}^a, D_{PEM}, D_{CL}^c, and D_{GDL}^c are the diffusion coefficients of H_2 in GDL(a), CL(a), PEM, CL(c), and GDL(c), respectively. Hence, D_{H_2} can be deduced from the rearrange-

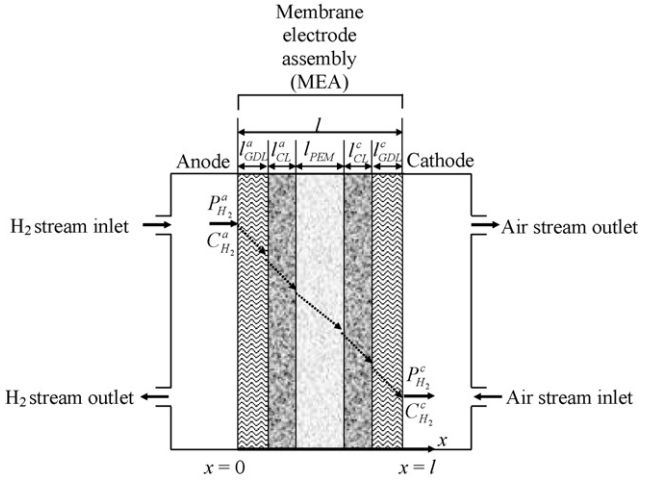

Fig. 1. Schematic diagram of hydrogen crossover through the (MEA) in a fuel cell.

ment of Eq. (5):

$$D_{H_2} = \frac{l^a_{GDL} + l^a_{CL} + l_{PEM} + l^c_{CL} + l^c_{GDL}}{(l^a_{GDL}/D^a_{GDL}) + (l^a_{CL}/D^a_{CL}) + (l_{PEM}/D_{PEM}) + (l^c_{CL}/D^c_{CL}) + (l^c_{GDL}/D^c_{GDL})} \quad (7)$$

Eq. (7) clearly indicates that the diffusion from every layer depicted in Fig. 1 contributes to the overall H_2 diffusion. Since H_2 diffused from the anode to the cathode would fully react with O_2 at the interface of PEM/CL(c), or would be completely oxidized electrochemically by the measurement procedure described in Section 2, the H_2 diffusion paths l^c_{CL} and l^c_{GDL} are equal to zero. Thus, Eq. (7) can be simplified as Eq. (8):

$$D_{H_2} = \frac{l^a_{GDL} + l^a_{CL} + l_{PEM}}{(l^a_{GDL}/D^a_{GDL}) + (l^a_{CL}/D^a_{CL}) + (l_{PEM}/D_{PEM})} \quad (8)$$

For the anode GDL and CL, the diffusion coefficients D^a_{GDL} and D^a_{CL} can be expressed as Eqs. (9) and (10), respectively, based on the Bruggeman correlation [28,29]

$$D^a_{GDL} = D^g_{H_2}[\varepsilon^a_{GDL}(1 - s^a_{GDL})]^\tau \quad (9)$$

$$D^a_{CL} = D^g_{H_2}[\varepsilon^a_{CL}(1 - s^a_{CL})]^\tau \quad (10)$$

where $D^g_{H_2}$ is the vapour-phase H_2 diffusion coefficient; its typical value at 80 °C is 2.63×10^{-2} cm^2 s^{-1} [28,29]. ε^a_{GDL} and ε^a_{CL} are the porosities of GDL and CL, respectively, and s^a_{GDL} and s^a_{CL} are the water saturation degrees inside GDL and CL, respectively. Their typical values are in the range of 0–1. τ is the tortuosity, which is often assumed to be 1.5.

Although D_{PEM} for Nafion membranes has been formulated empirically as a function of temperature (T) in the literature [30], the backpressure (P) and RH dependences measured in a fuel cell environment should be closer to a real situation.

Based on the literature, the typical thicknesses of PEMs are ~50 μm for Nafion 112 and ~175 μm for Nafion 117. The thickness for GDL is about 200 μm. The diffusion coefficients of H_2 crossover through GDL(a), CL(a), and PEM layers for a conventional MEA in a fuel cell at 80 °C are at the orders of ~10^{-2} cm^2 s^{-1}, ~10^{-4} cm^2 s^{-1}, and ~10^{-6} cm^2 s^{-1}, respectively. Combining these values into Eq. (8), it can be seen that the H_2 crossover through an MEA is predominantly caused by the membrane diffusion, which is mainly due to the smallest D_{PEM} value. The contributions from both GDL and CL diffusions can be ignored. Therefore, Eq. (8) can be simplified further to be Eq. (11) by eliminating the contributions of GDL(a), and CL(a):

$$\frac{l}{D_{H_2}} = \frac{l_{PEM}}{D_{PEM}} \quad (11)$$

Eq. (11) indicates that the overall diffusion coefficient value of H_2 crossover (or diffusion) through the MEA, obtained experimentally, is equal to that through the PEM. This has been recognized widely in the literature. For example, the dependence of H_2 crossover on the membrane thickness was confirmed by Kocha et al. [15], who compared the H_2 crossover currents measured in Nafion 112 and in Nafion 111 in the temperature range of 25–80 °C, suggesting that the dominant factor limiting the H_2 crossover rate is the membrane diffusion coefficient.

Combining Eq. (11) with Eq. (4), the H_2 crossover rate can be expressed as Eq. (12) if the crossed H_2 at the cathode can be completely oxidized ($C^c_{H_2} = 0$):

$$J^{cross}_{H_2} = \left(\frac{D_{PEM}}{l_{PEM}}\right) C^a_{H_2} \quad (12)$$

Eq. (12) suggests that the H_2 crossover rate through the MEA is equal to that through the PEM. An alternative expression for Eq. (12) can be introduced as Eq. (13):

$$J^{cross}_{H_2} = \left(\frac{K^{PEM}_{H_2} D_{PEM}}{l_{PEM}}\right) P^a_{H_2} \quad (13)$$

where $K^{PEM}_{H_2}$ is a H_2 partial pressure-related solubility coefficient in the PEM with a unit of mol cm^{-3} atm^{-1}, and $P^a_{H_2}$ is the H_2 partial pressure in the anode feed stream with a unit of atm. The product of the solubility ($K^{PEM}_{H_2}$) and diffusivity (D_{PEM}) can be defined as the permeability coefficient of H_2 in the PEM, $\psi^{PEM}_{H_2}$, with a unit of mol cm^{-1} atm^{-1} s^{-1}:

$$\psi^{PEM}_{H_2} = K^{PEM}_{H_2} D_{PEM} \quad (14)$$

Eq. (15) is obtained by substituting Eq. (14) into Eq. (13):

$$J^{cross}_{H_2} = \left(\frac{\psi^{PEM}_{H_2}}{l_{PEM}}\right) P^a_{H_2} \quad (15)$$

Similar to D_{H_2} (or D_{PEM}), $\psi^{PEM}_{H_2}$ is also a function of T, P, RH, water content, and the nature of the membrane [21]. For a defined fuel cell system, the value of l_{PEM} in Eq. (15) does not vary substantially; the other two factors, $\psi^{PEM}_{H_2}$ and $P^a_{H_2}$, may become more dominate to influence H_2 crossover, as suggested by Eq. (15).

The permeability coefficient, ψ_{H_2}, can then be determined by rearranging Eq. (15):

$$\psi^{PEM}_{H_2} = \frac{J^{cross}_{H_2} l_{PEM}}{P^a_{H_2}} \quad (16)$$

In Eq. (16), the values of $J^{cross}_{H_2}$ and $P^a_{H_2}$ can be measured experimentally, and then $\psi^{PEM}_{H_2}$ can be calculated at different Ts, Ps, and RHs if l_{PEM} is known (for Nafion 112, l_{PEM} = 50 μm; for Nafion 117, l_{PEM} = 175 μm).

3.2. H_2 crossover rate as a function of T, P, and RH

As described in Section 2, hydrogen crossover was measured using a steady-state electrochemical method. The current induced by crossed-over hydrogen ($I^{cross}_{H_2}$) was used to simulate the values of $\psi^{PEM}_{H_2}$ at various conditions. Table 1 lists the H_2 crossover rates obtained at various Ts, Ps, and RHs using a Nafion 112-based MEA. In general, the magnitude of $J^{cross}_{H_2}$ goes up monotonically with increases in temperature and backpressure. However, the RH effect is more complicated than those of temperature and backpressure.

Table 1
Measured H_2 crossover rate at various temperatures, backpressures, and relative humidities using a Nafion 112-based MEA

Temperature (°C)	RH (%)	Measured H_2 crossover rate (mol cm^{-2} s^{-1})		
		3.04[a]	2.02[a]	1.00[a]
80	100	2.04E−08	1.30E−08	3.78E−09
	70	1.91E−08	1.20E−08	4.14E−09
	50	1.80E−08	1.16E−08	4.51E−09
	25	1.74E−08	1.14E−08	5.30E−09
100	100	2.69E−08	1.48E−08	4.13E−09
	70	2.82E−08	1.43E−08	5.91E−09
	50	2.57E−08	1.35E−08	7.00E−09
	25	2.23E−08	1.42E−08	8.23E−09
120	100	3.05E−08	1.65E−08	8.13E−09
	70	4.16E−08	2.33E−08	1.19E−08
	50	5.02E−08	2.90E−08	1.61E−08
	25	6.28E−08	4.26E−08	2.17E−08

The thickness of the Nafion 112 was adopted as 50 μm.
[a] Backpressure (atm).

3.2.1. Temperature effect on the H_2 crossover rate

All the data listed in Table 1 follow a trend in which the H_2 crossover rate increases with increasing temperature. This observation has also been reported in the temperature range of 60–80 °C, and was explained according to the increase in membrane flexibility when the temperature and humidity were increased [8]. Because the permeability coefficient, $\psi_{H_2}^{PEM}$, is directly related to the H_2 solubility and diffusion coefficients [15], any effect of temperature on these two coefficients could cause a change of $\psi_{H_2}^{PEM}$ The increase of $\psi_{H_2}^{PEM}$ with increasing temperature probably indicates that the effect of temperature on the diffusion coefficient is more significant than that on the solubility coefficient.

3.2.2. Backpressure effect on the H_2 crossover rate

Fig. 2 shows the H_2 crossover rate as a function of backpressure at 50% RH and three different temperatures. A monotonic increase in the H_2 crossover rate with increasing backpressure can be observed. It is understandable that an increase in backpressure will result in a H_2 partial pressure increase, which then creates a larger pressure difference across the PEM. As expected by Eq. (15), the H_2 crossover rate, $J_{H_2}^{cross}$, will be increased if the H_2 partial pressure, $P_{H_2}^{a}$, increases.

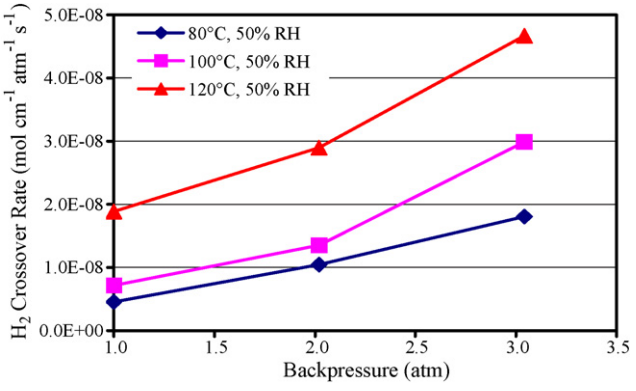

Fig. 2. H_2 crossover rate as a function of fuel cell backpressure at 50% relative humidity and three different temperatures as marked in the figure. Nafion 112-based MEA with an active area of 4.4 cm^2. Anode H_2 stream flowrate: 0.1 L min^{-1}; cathode N_2 stream flowrate: 0.5 L min^{-1}. Cathode potential: 0.5 V vs. anode hydrogen electrode.

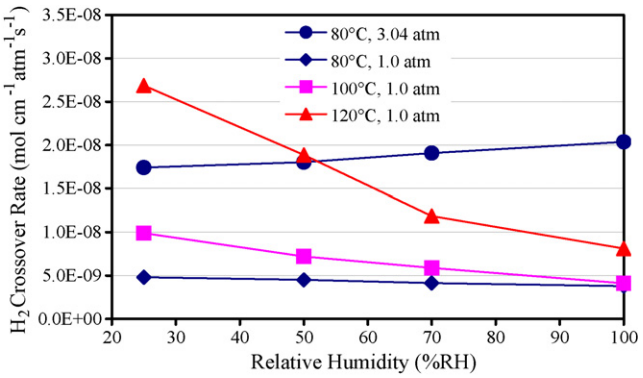

Fig. 3. H_2 crossover rate as a function of relative humidity in fuel cell anode feed stream at three different temperatures as marked in the figure. Nafion 112-based MEA with an active area of 4.4 cm^2. Anode H_2 stream flowrate: 0.1 L min^{-1}; cathode N_2 stream flowrate: 0.5 L min^{-1}. Cathode potential: 0.5 V vs. anode hydrogen electrode.

3.2.3. RH effect on the H_2 crossover rate

Fig. 3 shows the typical data obtained regarding the RH effect on the H_2 crossover rate. It seems that the RH effect is more complicated than those of temperature and backpressure. For example, at 80 °C and 3.0 atm, the H_2 crossover rate increases as the RH increases, while at the same temperature and a backpressure of 1.0 atm, the RH increase reduces the crossover rate. However, at high temperatures (120 °C), the effect of RH on H_2 crossover is always negative; that is, the H_2 crossover is reduced with increasing RH.

For a fuel cell anode feed stream, the inlet total pressure is the sum of the H_2 partial pressure and the water vapour partial pressure ($P_{H_2O}^{a}$):

$$P_{H_2\text{-inlet}}^{a} = P_{H_2}^{a} + P_{H_2O}^{a} \quad (17)$$

For a controlled total pressure, an increase in the RH level results in an increase in the magnitude of $P_{H_2O}^{a}$. Consequently, the $P_{H_2}^{a}$ is reduced accordingly, as expected from Eq. (17). It can be seen from Eq. (15) that the H_2 crossover will be reduced if $P_{H_2}^{a}$ is decreased, which is the case at 100 °C and 120 °C, as shown in Fig. 3. However, the increasing RH level will increase the water content in the membrane, which may cause changes in both the value of H_2 solubility and the diffusion coefficients. At lower temperature (80 °C), the value increase in the permeability coefficient caused by an RH increase could be greater than that caused by a $P_{H_2}^{a}$ reduction, resulting in the increasing trend observed in Fig. 3 (80 °C, 3.04 atm).

3.3. H_2 permeability coefficient as a function of T, P, and RH

The data in Table 2 were obtained using Eq. (16) based on the measured data of H_2 crossover rate and partial pressure. Table 2 indicates that an increase in temperature can effectively increase

Table 2
Calculated H_2 permeability coefficients at various temperatures, backpressures, and relative humidities used a Nafion 112-based MEA

Temperature (°C)	RH (%)	H_2 permeability coefficient (mol cm^{-1} atm^{-1} s^{-1})		
		3.04[a]	2.02[a]	1.00[a]
80	100	3.87E−11	3.71E−11	1.88E−11
	70	3.47E−11	3.24E−11	1.93E−11
	50	3.10E−11	2.95E−11	2.06E−11
	25	2.93E−11	2.80E−11	2.21E−11
100	100	6.13E−11	5.24E−11	2.40E−11
	70	5.74E−11	4.42E−11	3.11E−11
	50	4.89E−11	3.84E−11	3.39E−11
	25	3.90E−11	3.64E−11	3.54E−11
120	100	1.04E−10	9.14E−11	6.94E−11
	70	1.08E−10	9.52E−11	7.94E−11
	50	1.12E−10	9.80E−11	8.95E−11
	25	1.18E−10	1.08E−10	1.01E−10

The thickness of the Nafion 112 was adopted as 50 μm.
[a] Backpressure (atm).

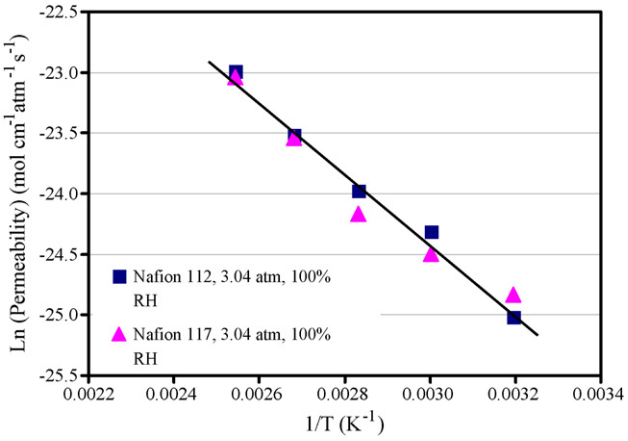

Fig. 4. Arrhenius plots of H_2 permeability coefficient for both Nafion 112 and Nafion 117-based MEAs at 3.04 atm backpressure and 100% RH in the temperature range of 40–120 °C. Both MEAs have an active area of 4.4 cm^2. Anode H_2 stream flowrate: 0.1 L min^{-1}; cathode N_2 stream flowrate: 0.5 L min^{-1}. Cathode potential: 0.5 V vs. anode hydrogen electrode.

the H_2 permeability coefficient at any given backpressure and RH. This trend was also observed by Kocha et al. [15]. Table 2 also shows that the temperature effect is much larger than those affected by backpressure and RH.

The temperature dependence of the permeability coefficient can be used to obtain the activation energy of H_2 permeability ($E_{H_2}^{PEM}$) through an Arrhenius relation:

$$\psi_{H_2}^{PEM} = \psi_{H_2}^{0}\, e^{-E_{H_2}^{PEM}/RT} \tag{18}$$

where $\psi_{H_2}^{0}$ is the maximum H_2 permeability coefficient (i.e., at infinite temperature), and R is the gas constant. Eq. (18) can be written into a logarithmic form:

$$\ln\psi_{H_2}^{PEM} = \ln\psi_{H_2}^{0} + \left(-\frac{E_{H_2}^{PEM}}{R}\right)\frac{1}{T} \tag{19}$$

Thus, a straight line is expected by plotting $\ln \psi_{H_2}^{PEM}$ against $1/T$, and the values of $\psi_{H_2}^{0}$ and $E_{H_2}^{PEM}$ can be evaluated from the intercept and slope of the plot, respectively. Fig. 4 gives the typical Arrhenius plots for both Nafion 112 and Nafion 117-based MEAs at 3.04 atm backpressure and 100% RH in the temperature range of 40–120 °C. Both Nafion 112 and Nafion 117 give similar values of activation energy and the maximum permeability coefficient, which are 24.7 kJ mol^{-1} and 1.39×10^{-7} mol cm^{-1} atm^{-1} s^{-1}, respectively. The value of $E_{H_2}^{PEM}$ is close to the value of 21.03 kJ mol^{-1} reported in the literature using Nafion 111 and Nafion 112 membranes [15]. The fact that the values of activation energy and maximum permeability obtained from Nafion 112 are similar to those obtained from Nafion 117 strongly suggests that the membrane thickness is not the dominating factor affecting the H_2 permeability coefficient. Yoshida et al. [20] also found that the $\psi_{H_2}^{PEM}$ alues for three types of Flemion membranes and Nafion 117 were nearly the same and were independent of the membrane thickness in the region from 15 to 230 μm at 70 °C. However, at 120 °C, the $\psi_{H_2}^{PEM}$ values were an order larger than those at 30 °C. Hence, the H_2 permeation coefficient is more strongly dependent on temperature than on membrane thickness.

Therefore, Eq. (18) can be rewritten as Eq. (20) for the operation conditions of backpressure 3.04 atm and 100% RH:

$$\psi_{H_2}^{PEM} = 1.39 \times 10^{-7}\, e^{-2980/T} \tag{20}$$

Table 2 shows that the permeability coefficient is also dependent on the backpressure and RH. Similar to the effect of temperature, increasing backpressure can always raise the value of the H_2 permeability coefficient at any given RH. However, the effect of RH on the permeability coefficient seems to be more complicated. For example, the trends obtained when RH is increased at lower temperatures (80 °C and 100 °C) and higher backpressures (2.02 atm and 3.04 atm) are opposite to those obtained at higher a temperature (120 °C) and lower pressure (1.0 atm). The change in the water content of the membrane at different backpressures and temperatures can affect both H_2 solubility and diffusivity, resulting in the change in the permeability coefficient. More work has been scheduled to investigate the mechanism of H_2 crossover through different membranes in order to improve our fundamental understanding of these effects.

For a simple approach, the effects of backpressure and RH were empirically simulated and can be expressed as Eq. (21):

$$\psi_{H_2}^{PEM} = 1.39 \times 10^{-7}\, e^{-(2980 f(P,RH))/T} \tag{21}$$

where $f(P, RH)$ reflects the effects of backpressure and RH on the activation energy. However, in order to obtain the exact expression for this $f(P, RH)$ by empirical simulation, a statistically significant amount of data is necessary, which is beyond the scope of this paper.

4. Conclusions

The hydrogen crossover in a PEM fuel cell environment was measured experimentally in the temperature range of 40–120 °C, focusing especially on the higher temperature range of 80–120 °C. An H_2 permeation model based on an MEA con-

sisting of five layers – anode GDL, anode CL, PEM, cathode GDL, and cathode CL – was constructed to obtain a simple expression for the calculation of H_2 permeability coefficients based on the measured H_2 crossover rates and controlled H_2 partial pressures at various temperatures, backpressures, and relative humidities. The model analysis suggests that the H_2 permeation through the PEM is a limiting step in the overall process.

The H_2 permeability coefficients obtained as a function of temperature, backpressure, and RH show that an increase in temperature can effectively increase the H_2 permeability coefficient at any given backpressure and RH. Similarly, increasing backpressure can always increase the value of the H_2 permeability coefficient at any given RH. However, the effect of RH on the permeability coefficient seems to be more complicated. The temperature effect is much larger than those caused by backpressure and RH. An equation to describe the T dependencies was obtained based on experimental data by simulation.

The activation energies and maximum permeability coefficients of H_2 permeation through both Nafion 112 and Nafion 117-based MEAs were evaluated separately. Both MEAs showed similar values for permeability coefficients and activation energies, suggesting that the membrane thickness has no significant effect on the H_2 permeation mechanism.

Acknowledgements

The authors would like to thank the financial support of the NRC National PEM Fuel Cell Program and the NRC Institute for Fuel Cell Innovation (NRC-IFCI). Discussion with Dr. Simon Liu and Dr Haijiang Wang are appreciated. Dr. Xuan Cheng also greatly appreciates the financial support of the China Scholarship Council and the National Natural Science Foundation of China (20433060) for the living allowances during her visit and stay at NRC-IFCI.

References

[1] J. St-Pierre, D.P. Wilkinson, AIChE J. 47 (2001) 1482.
[2] C. Song, Y. Tang, J.L. Zhang, J. Zhang, H. Wang, J. Shen, S. McDermid, J. Li, P. Kozak, Electrochim. Acta 52 (2007) 2552.
[3] Y. Tang, J. Zhang, C. Song, H. Liu, J. Zhang, H. Wang, S. Mackinnon, T. Peckham, J. Li, S. McDermid, P. Kozak, J. Electrochem. Soc. 153 (2006) A2036–A2043.
[4] http://www.hstrading.co.kr/products/data/ion-1.pdf.
[5] J. Zhang, Y. Tang, C. Song, J. Zhang, H. Wang, J. Power Sources 163 (2006) 532.
[6] A. Collier, H. Wang, X. Zi Yuan, J. Zhang, D.P. Wilkinson, Int. J. Hydrogen Energy 31 (2006) 1838.
[7] J. Yu, T. Matsuura, Y. Yoshikawa, M.N. Islam, M. Hori, Electrochem. Solid-State Lett. 8 (2005) A156–A158.
[8] M. Inaba, T. Kinumoto, M. Kiriake, R. Umebayashi, A. Tasaka, Z. Ogumi, Electrochim. Acta 51 (2006) 5746.
[9] K. Teranishi, K. Kawata, S. Tsushima, S. Hirai, Electrochem. Solid-State Lett. 9 (2006) A475–A477.
[10] H.L. Yeager, A. Steck, J. Electrochem. Soc. 128 (1981) 1880.
[11] Y. Song, J.M. Fenton, H.R. Kunz, L.J. Bonville, M.V. Williams, J. Electrochem. Soc. 152 (2005) A539–A544.
[12] T. Sakai, H. Takenaka, E. Torikai, J. Electrochem. Soc. 133 (1986) 88.
[13] Z. Ogumi, Z. Takehara, S. Yoshizawa, J. Electrochem. Soc. 131 (1984) 769.
[14] Z. Ogumi, T. Kuroe, Z.-i. Takehara, J. Electrochem. Soc. 132 (1985) 2601.
[15] S.S. Kocha, J.D. Yang, J.S. Yi, AIChE J. 52 (2006) 1916.
[16] R. Jiang, H.R. Kunz, J.M. Fenton, J. Power Sources 150 (2005) 120.
[17] N. Yoshida, T. Ishisaki, A. Watakabe, M. Yoshitake, Electrochim. Acta 43 (1998) 3749.
[18] S. Kocha, P. Plasse, L. Onishi, D. Wheeler, J. Bett, Pre-Print Archive – American Institute of Chemical Engineers, [Spring National Meeting], New Orleans, LA, United States, Mar. 11–14, 2002.
[19] J. Zhang, Z. Xie, J. Zhang, Y. Tang, C. Song, T. Navessin, Z. Shi, D. Song, H. Wang, D.P. Wilkinson, J. Power Sources 160 (2006) 872.
[20] T.E. Springer, T.A. Zawodzinski, S. Gottesfeld, J. Electrochem. Soc. 138 (1991) 2334.
[21] A.Z. Weber, J. Newman, J. Electrochem. Soc. 151 (2004) A311–A325.
[22] P. Rama, R. Chen, R. Thring, IMechE Part A: J. Power Energy 220 (2006) 535.
[23] Y. Si, H. Russell Kunz, J.M. Fenton, J. Electrochem. Soc. 151 (2004) A623–A631.
[24] V. Ramani, H.R. Kunz, J.M. Fenton, J. Membr. Sci. 266 (2005) 110.
[25] H.L. Yeager, ACS Symp. Ser. 180 (1982) 41.
[26] T.D. Gierke, W.Y. Hsu, ACS Symp. Ser. 180 (1982) 283.
[27] K. Broka, P. Ekdunge, J. Appl. Electrochem. 27 (1997) 117.
[28] K.Z. Yao, K. Karan, K.B. McAuley, P. Oosthuizen, B. Peppley, T. Xie, Fuel Cells 4 (2004) 3.
[29] A.C. West, T.F. Fuller, J. Appl. Electrochem. 26 (1996) 557.
[30] R.S. Yeo, J. McBreen, J. Electrochem. Soc. 126 (1979) 1682.